Fibril Formation by Triblock Copolymers of Silklike β-Sheet Polypeptides and Poly(ethylene glycol)

Jurgen M. Smeenk, Peter Schön, Matthijs B. J. Otten, Sylvia Speller, Hendrik G. Stunnenberg, and Jan C. M. van Hest*

Institute for Molecules and Materials, Organic Chemistry Department, Radboud University Nijmegen, Toernooiveld 1, 6525 ED Nijmegen, The Netherlands

Received October 6, 2005; Revised Manuscript Received February 23, 2006

ABSTRACT: A series of ABA triblock copolymers consisting of a central β-sheet polypeptide block and poly(ethylene glycol) (PEG) end blocks were constructed in order to investigate the effect of PEG chain length on assembly behavior. The polypeptide block, consisting of tandem repeats of -$(AG)_3$EG- (A = alanine, G = glycine, and E = glutamic acid), was prepared by *E. coli* expression and subsequently conjugated via two flanking cysteine residues to maleimide-functionalized PEGs of various chain length. Infrared spectroscopy showed that no major effect of PEG chain length on polypeptide folding occurred. With atomic force microscopy a fibrillar microstructure was observed for all conjugates, with fibrillar heights of ∼2 nm. Only at the highest molecular weight of PEG (5000 g/mol) could an influence on assembly be noticed by the appearance of shorter fibers when compared to the hybrid block copolymers containing the lower molecular weight PEG chains. It can be concluded that this class of peptide-based materials is well capable of fibril formation in the β-sheet stacking direction, whereas the PEG chains prevent their further side-to-side aggregation without interfering strongly with the desired β-sheet interactions.

Introduction

Peptides and proteins are actively being used as building blocks for the fabrication of higher order nanostructures via self-assembly. Knowledge of the relationship between primary amino acid sequence and folding behavior as well as an increasing insight into protein−protein interactions makes them attractive candidates for the creation of functional nanostructured materials. Naturally occurring proteins with an inherent property to self-assemble have been used to construct new materials. A variety of such systems have been investigated, such as bacterial S-layer proteins[1] and the yeast prion protein Sup35p.[2] S-layer proteins are crystalline two-dimensional protein arrays at the cell surface of certain bacteria. Because of the presence of defined pores, they have been used e.g. for ultrafiltration and as template for the deposition of regularly arranged metal nanoparticles.[1] Yeast prion protein fibrils have been used for the preparation of conducting nanowires by selective metal deposition.[2]

Alternatively, new assemblies have been created by "polyvalent design",[3] using oligomeric proteins in combination with multivalent ligands. An example is the formation of a "diamond-like" lattice resulting from the binding of the tetrameric protein concanavalin A and a two-headed carbohydrate molecule.[4] Two-dimensional networks with controllable mesh size could be created by using a tetrameric aldolase conjugated with biotin in combination with streptavidin as a rigid linker.[5]

Besides building blocks of known assembly behavior, "de novo designed" peptide or protein building blocks have become increasingly important for the construction of new self-assembling systems. Especially, small peptides forming β-strands and β-hairpins, which can be synthesized easily by solid-phase synthesis, have been investigated for their assembly properties. Simple design principles can be applied, such as amphiphilicity in β-strands by the alternation of polar and nonpolar residues, interruption of hydrogen bonding and formation of turns by the use of proline, charge arrangement in the β-strands, and formation of salt bridges. These factors together determine the orientation of β-strands and the shape of the resulting aggregates and offer in addition the opportunity to introduce stimulus responsiveness. A variety of architectures such as ribbons,[6,7] nanotubes,[8,9] monolayers with nanoscale order,[10−12] gels,[13,14] and membranes[15] have been reported for β-sheet peptides. These systems may be used e.g. as scaffolds for tissue engineering or in targeted drug delivery.[16]

Higher molecular weight designed β-sheet polypeptides have been prepared using molecular biology techniques via expression of a series of synthetic genes coding for seven-residue long amphiphilic β-strands, separated by turn sequences.[17] All of them assembled into fibrils and could form monolayers at the air−water interface[18] or flat sheets on highly oriented pyrolytic graphite (HOPG).[19] The gelation properties of the high molecular weight repetitive β-sheet fibril forming sequence poly(AEAEAKAK) has been reported by Muller and co-workers.[20] Interestingly, they showed that the fibrils were of similar diameter as the low molecular weight analogues[15] but that high molecular weight material was more elastic.

Despite the large amount of research that is performed on peptide and protein assembly, relatively few reports have described the self-assembly of hybrid block copolymers, i.e., copolymers which combine traditional synthetic polymers with peptide sequences. These kinds of block copolymers have the potential to combine properties of the peptide block, such as assembly, recognition, or bioactivity, with the specific chemical and physical properties of synthetic polymers, such as reactivity and solubility. Most reported hybrid block copolymers are composed of a synthetic polymer combined with either a homopolypeptide sequence prepared via ring-opening polymerization of an *N*-carboxyanhydride[21,22] or a small peptide prepared via solid-phase synthesis. In particular, the latter

* Corresponding author: Tel +31 (0)24 365 3204; Fax +31 (0)24 365 33 93; e-mail j.vanhest@science.ru.nl.

10.1021/ma0521654 CCC: $33.50
Published on Web 03/18/2006

approach is of interest for self-assembly. Meredith and co-workers reported the formation of fibrils of a diblock copolymer consisting of the amyloid-β(10-35) peptide and poly(ethylene glycol) (PEG).[23,24] Side-to-side aggregation of fibrils was hindered by the PEG-coated surface of the fibrils. The assembly behavior of hybrid block copolymers consisting of PEG and amphiphilic β-strand peptide sequences was investigated by Klok and co-workers.[25,26] These hybrids formed superstructures consisting of alternating PEG layers and peptide domains in an antiparallel β-sheet conformation in the solid-state and fibrillar structures after assembly in water. Silklike multiblock copolymers of PEG and the β-sheet forming sequences AGAG (A = alanine, G = glycine) and poly(alanine) based on silkworm and spider silk, respectively, were reported by Sogah and co-workers.[27,28] A microphase-separated architecture of peptide domains (20−200 nm) dispersed in a continuous PEG phase was observed for these polymers.

Recently, we have reported on an approach in which a recombinantly produced, designed protein polymer was combined with the synthetic polymer PEG.[29] The protein polymer block consisted of tandem repeats of the amino acid sequence -$(AG)_3$EG- (E = glutamic acid). The feasibility of controlling the solid-state structure of polymeric materials based on this sequence was already shown by Tirrell and co-workers.[30] The regular interspersion of the β-strand-forming alanylglycine repeats with glutamic acid residues resulted in controlled crystallization from aqueous formic acid, leading to folded-chain lamellar crystals with the polar and bulky glutamic acid residues confined to the crystal surface.[31−33] Although control over folding of the polypeptide chain was demonstrated, crystallization resulted in large extended-plate-like structures. In our approach control over the assembly process of these β-sheet structures was obtained by preparation of triblock copolymers consisting of the β-sheet polypeptide as central block in combination with two PEG end blocks. The attachment of the flanking PEG chains blocked the formation of platelike crystals and resulted in assembly into well-defined fibrils.

In this article we report on the preparation and characterization of a series of different PEG β-sheet conjugates, in which the ratio between peptide and polymer part is varied. The rationale behind this study was to determine to what extent fibril formation of the β-sheet polypeptides is affected by the attachment of synthetic polymers of varying molecular weight. Therefore, the β-sheet polypeptide $[(AG)_3EG]_{10}$ was coupled to PEG chains of M_n = 750, 2000, and 5000 g mol^{-1}, and the effect of PEG chain length, and thus radius of gyration (R_g), on β-sheet formation and assembly properties was investigated. By increasing the molecular weight of PEG from 750 to 5000 g mol^{-1}, an increase in R_g and therefore steric hindrance would be expected, which should lead to a reduced propensity to self-assemble.

Experimental Section

General Methods. Ni-NTA and gel filtration chromatography were performed using a Biologic FPLC instrument (BioRad). ^{1}H NMR spectra were recorded on a Varian Inova-400 instrument at 298 K. Chemical shifts are reported in ppm relative to tetramethylsilane (δ = 0.00 ppm) or the appropriate solvent signal. ^{13}C NMR spectra were recorded on a Bruker AC-300 instrument at 298 K.

MALDI-TOF mass spectra were measured on a Bruker Biflex III spectrometer. Freeze-dried products were dissolved in 1:1 (v/v) water:acetonitrile with 0.1% trifluoroacetic acid to a final concentration of 10 mg mL^{-1} and mixed in a 1:1 ratio with a solution of 20 mg mL^{-1} of sinapinic acid (Sigma) in the same solvent and spotted on a MALDI plate.

SDS-PAGE and Immunoblot Analysis. SDS-PAGE and immunoblot analysis was carried out according standard procedures.[34] For immunoblot analysis protein samples were separated on 15% SDS-PAGE gel and transferred to nitrocellulose membrane. Membranes were incubated in TBST (10 mM Tris, pH 8.0, 150 mM NaCl, 0.1% Tween 20) containing 5% nonfat milk powder for 1 h and then incubated with T7-tag mouse monoclonal antibody (Novagen; 1:10 000) in 5% milk powder in TBST overnight at 4 °C. The blots were washed three times for 10 min with TBST at room temperature followed by incubation with rabbit-anti-mouse peroxidase (Dako Diagnostics; 1:2000) for 1 h. The blots were washed three times for 5 min with TBST at room temperature and dried with Whatmann paper. The blots were developed using the ECL chemiluminescent detection reagents (Amersham Biosciences). The detection solution was prepared by mixing equal volumes of solution 1 and 2 on a glass plate, and the blot was placed with the protein containing side down on top of this solution for 30 s. After drying with Whatmann paper, the blot was enclosed in plastic wrap and exposed to film (Kodak chemiluminescence film) for 30 s.

Ellman's Assay for Determination of Free Thiols.[35] To 50 μL of protein solution of suitable concentration was added 950 μL of 100 mM NaH_2PO_4 buffer (pH 6.8) containing 150 mM NaCl and 1 mM EDTA. To this solution was added 50 μL of 3 mM 5,5′-dithiobis(2-nitrobenzoic acid) (DTNB; Sigma; dissolved in the same buffer). The absorbance difference between the protein sample and a reference without protein was measured at 412 nm (ϵ_{412} = 10 900 M^{-1} cm^{-1}).

Methanol-Induced Crystallization. Crystallization of the conjugates was induced by vapor diffusion of methanol (p.a. Merck) into a solution of 1 or 10 mg mL^{-1} conjugate in 70% formic acid (Merck). Thereto, an Eppendorf tube containing the conjugate solution was placed in a Duran bottle filled with 20 mL of methanol. The bottle was closed and incubation was carried out for 2 days.

Fourier Transform Infrared Spectroscopy. Transmission-FTIR spectra were measured with a Thermo Mattson Genesis IR-300 spectrometer using a deuterated triglycine sulfate detector (resolution, 4 cm^{-1}; number of scans, 64). Samples were allowed to dry on the surface of a Ge ATR crystal prior to measurement.

Transmission Electron Microscopy. All samples were prepared on copper specimen grids covered with a carbon support film (CF200-Cu; Electron Microscopy Sciences, Washington). The grids were placed with the carbon film down on top of a 5 μL droplet of protein suspension (1 mg mL^{-1}) in methanol or on a gel (10 mg mL^{-1}) for 30 s. The grids were allowed to dry and were subsequently shadowed with platinum at an elevation angle of 45°. Images were recorded using a JEOL JEM 1010 microscope (60 kV) equipped with a CCD camera.

Atomic Force Microscopy. Solutions of the conjugate diluted with methanol to concentrations of 10−100 μg mL^{-1} were applied onto a freshly cleaved mica surface by drop-casting. The morphologies of the samples were analyzed by means of tapping-mode AFM with a Nanoscope IIIa instrument operating in air at room temperature. Height and phase images were recorded with microfabricated silicon cantilevers (length 100 mm and width 35 mm) that had a spring constant of 5.5−22.5 N m^{-1}, using scan rates of 1−2 lines s^{-1} and a resolution of 512 × 512 pixels.

Expression and Purification of $[(AG)_3EG]_{10}$ (1). The expression and purification of $[(AG)_3EG]_{10}$ were carried out as described previously.[29] An isolated yield was 6 mg per liter of culture. MS (MALDI-TOF): m/z = 11 134 Da (calculated mass: 11 082 Da).

Synthesis of Maleimide-Functionalized PEGs. PEGs monofunctionalized with an amine group with molecular weights of 750, 2000, and 5000 g mol^{-1} were purchased from Rapp Polymere GmbH (Tübingen, Germany). ϵ-Maleimidocaproic acid (Sigma), benzotriazole-1-yl-oxytris(dimethylamino)phosphonium hexafluorophosphate (BOP) (Advanced Chemtech), diisopropylethylamine (Fluka), sodium 2-mercaptoethanesulfonate (Sigma), and 5,5′-dithiobis(2-nitrobenzoic acid) (Sigma) were used as received. Thin-layer chromatography analyses were performed on Merck precoated silica gel 60 F254 plates (layer thickness 0.25 mm) using the solvent mixtures indicated. Maleimide derivatives were detected according

to a literature procedure[36] after TLC separation by spraying the thin-layer plates with a 0.1% solution of 5,5′-dithiobis(2-nitrobenzoic acid) in 1:1 ethanol−Tris-HCl buffer (pH 8.2) and then with a 2% solution of sodium 2-mercaptoethanesulfonate in 80% ethanol until the background was bright yellow. Maleimide derivatives appeared as white spots. Product purification was performed with a Sephadex LH-20 gel filtration resin obtained from Amersham Biosciences.

*Maleimide-Functionalized PEG-750 (**2a**).* 391 mg of PEG-750-NH_2 (0.52 mmol) was dried by azeotropic evaporation with benzene. The dried product was dissolved in 5 mL of DMF together with 110 mg of ϵ-maleimidocaproic acid (0.52 mmol), 230 mg of BOP coupling reagent (0.52 mmol), and 192 mg of diisopropylethylamine (1.60 mmol). After 24 h stirring at room temperature DMF was evaporated, and the resulting solid was redissolved in dichloromethane. This solution was subsequently extracted with 1 N HCl (twice), water, 5% $NaHCO_3$ (twice), water, and saturated NaCl. After evaporation the product was further purified by gel filtration chromatography using methanol/dichloromethane 1:1 v/v as eluent. The final yield was 217 mg of pure product (0.35 mmol, 68%). R_f = 0.60−0.75 (methanol/chloroform = 1:4 v/v, maleimide detection). ^{1}H NMR (400 MHz, $CDCl_3$): δ = 6.69 (s, 2H, C*H*═C*H*), 6.27 (br s, 1H, N*H*CO), 3.61−3.68 (br m, 68H, O(CH_2)$_2$O), 3.55 (t, 2H, CH_2CH$_2$NHCO), 3.51 (t, 2H, NCH_2), 3.44 (m, 2H, CH_2-NHCO), 3.38 (s, 3H, CH_3O), 2.17 (t, 2H, CH_2CONH), 1.66 (m, 2H, NHCOCH$_2$CH_2), 1.60 (m, 2H, CH_2CH$_2$N), 1.31 (m, 2H, CH$_2$CH_2CH$_2$CH$_2$N). ^{13}C NMR (75 MHz, $CDCl_3$): δ = 172.1 (1C, *C*ONH), 163.8 (2C, N*C*O), 133.5 (2C, *C*═*C*), 71.6 (1C, *C*H$_2$CH$_2$-NH), 70.2 (30C, O(*C*H$_2$)$_2$O), 58.7 (1C, *C*H$_3$O), 38.9 (1C, *C*H$_2$NH), 37.5 (1C, *C*H$_2$N), 36.1 (1C, *C*H$_2$CONH), 28.1 (1C, *C*H$_2$CH$_2$N), 26.2 (1C, CH$_2$*C*H$_2$CH$_2$), 24.9 (1C, *C*H$_2$CH$_2$CONH); MS (MALDI-TOF): Calcd for n = 15, $C_{43}H_{80}N_2O_{19}$ $[M + Na]^+$: 952.05; found m/z = 951.70. M_n(MALDI-TOF) = 1045, PDI = 1.01.

*Maleimide-Functionalized PEG-2000 (**2b**).* The maleimide functionalization and subsequent purification were carried out analogous to the route described for PEG-750. The reaction was performed with 800 mg of PEG-2000-NH_2 (0.4 mmol), 85 mg of ϵ-maleimidocaproic acid (0.4 mmol), 177 mg of BOP (0.4 mmol), and 155 mg of DIPEA (1.2 mmol). The final yield after gel filtration chromatography (Sephadex LH-20; methanol/dichloromethane 1:1 v/v as eluent) was 784 mg (0.36 mmol, 89%). R_f = 0.50−0.65 (methanol/chloroform = 1:5 v/v, maleimide detection). ^{1}H NMR (400 MHz, $CDCl_3$): δ = 6.69 (s, 2H,C*H*═C*H*), 6.20 (br s, 1H, N*H*CO), 3.61−3.68 (br m, 188H, O(CH_2)$_2$O), 3.55 (t, 2H, CH_2CH$_2$NHCO), 3.51 (t, 2H, NCH_2), 3.44 (m, 2H, CH_2NHCO), 3.38 (s, 3H, CH_3O), 2.17 (t, 2H, CH_2CONH), 1.66 (m, 2H, NHCOCH$_2$CH_2), 1.60 (m, 2H, CH_2CH$_2$N), 1.31 (m, 2H, CH$_2$CH_2CH$_2$CH$_2$N). MS (MALDI-TOF): Calcd for n = 48, $C_{109}H_{212}N_2O_{52}$ $[M + H]^+$: 2383.72; found m/z = 2383.13. M_n(MALDI-TOF) = 2325, PDI = 1.02.

*Maleimide-Functionalized PEG-5000 (**2c**).* The maleimide functionalization and subsequent purification were carried out analogous to the route described for PEG-750. The reaction was performed with 850 mg of PEG-5000-NH_2 (0.17 mmol), 36 mg of ϵ-maleimidocaproic acid (0.17 mmol), 75 mg of BOP (0.17 mmol), and 66 mg of DIPEA (0.51 mmol). The final yield after gel filtration chromatography (Sephadex LH-20; methanol/dichloromethane 1:1 v/v as eluent) was 617 mg (0.12 mmol, 70%). R_f = 0.50−0.65 (methanol/chloroform = 1:5 v/v, maleimide detection). ^{1}H NMR (400 MHz, $CDCl_3$): δ = 6.69 (s, 2H,C*H*═C*H*), 6.20 (br s, 1H, N*H*CO), 3.60−3.67 (br m, 460H, O(CH_2)$_2$O), 3.55 (t, 2H, CH_2-CH$_2$NHCO), 3.51 (t, 2H, NCH_2), 3.44 (m, 2H, CH_2NHCO), 3.38 (s, 3H, CH_3O), 2.17 (t, 2H, CH_2CONH), 1.66 (m, 2H, NHCOCH$_2$CH_2), 1.60 (m, 2H, CH_2CH$_2$N), 1.31 (m, 2H, CH$_2$CH_2-CH$_2$CH$_2$N). M_n(MALDI−TOF) = 5346, PDI = 1.01.

Conjugation of [(AG)$_3$EG]$_{10}$ with Poly(ethylene glycols) and ϵ-Maleimidocaproic Acid. 10 mg of protein was dissolved in 5 mL of 20 mM NaH_2PO_4 buffer (pH 8.0) containing 150 mM NaCl, 1 mM EDTA, and 200 mM dithiotreitol (DTT; Sigma) and incubated for 1 h at room temperature. To remove the excess of DTT, the protein was precipitated with trichloroacetic acid (TCA; Sigma) using a protocol adapted from Maniatis.[37] Precipitation by addition of 0.25 volumes of ice-cold 100% TCA was followed by incubation at −20 °C for 30 min. After centrifugation at 13 000 rpm for 10 min at 4 °C, the pellet was washed with 2.5 mL of ice-cold 20% TCA, followed by a second wash with 2.5 mL of 1% TCA. After each wash the solution was centrifuged for 5 min at 4 °C. The pellet was redissolved in 5 mL of 100 mM NaH_2PO_4 buffer (pH 6.8) containing 150 mM NaCl. For complete PEGylation of the cysteine residues a 5-fold excess of maleimide-functionalized PEG was immediately added as a 5 mL solution in the same buffer. For conjugation with ϵ-maleimidocaproic acid also 5 equiv was used. The reaction mixture was incubated overnight on a rotating arm.

Ni-NTA chromatography was used to remove the excess PEG or ϵ-maleimidocaproic acid.. The Ni-NTA beads were preequilibrated in 100 mM NaH_2PO_4 buffer (pH 8.0) containing 150 mM NaCl. The PEG conjugation solution was added to 10 mL of equilibrated 50% Ni-NTA suspension and incubated for 1 h at room temperature. The suspension was centrifuged for 5 min at 1500 rpm, and the supernatant was removed. Wash buffer (10 mL of 100 mM NaH_2PO_4 (pH 8.0), 150 mM NaCl) was added, and a column was loaded. The agarose beads were washed until all the PEG was removed (monitored by measuring absorption profile at 214 nm). Subsequently, the protein−PEG conjugate was eluted by increasing the imidazole concentration to 200 mM. Finally, the product was dialyzed against demi-water using a dialysis membrane (Spectra Por dialysis tubing, 3.5 kDa molecular weight cutoff) for 2 days and lyophilized.

*[(AG)$_3$EG]$_{10}$-PEG-750 Conjugate (**3a**).* ^{1}H NMR (400 MHz, H_2O/D_2O 9:1 v/v): The following major signals were assigned: δ = 1.40 (d, 123H, Ala-Hβ), 2.11 (m, 26H, Glu-Hβ), 2.31 (m, 26H, Glu-Hγ), 3.39 (s, 6H, CH_3O), 3.72 (s, 136H, O(CH_2)$_2$O), 3.97 (s, 92H, Gly-Hα), 4.34 (m, 54H, Ala/Glu-Hα). MALDI-TOF: m/z = 13 280 Da (calculated mass for bifunctionalized product: 13 202 Da), main signal. Furthermore, two small peaks were observed corresponding to monofunctionalized polypeptide (calculated mass: 12 157 Da, observed: m/z = 12 317 Da) and trifunctionalized polypeptide (calculated mass 14 247, observed m/z = 14 315 Da). Trifunctionalization is most likely the result of functionalization of lysine residues or the N-terminus, since the maleimide functionality eventually also reacts with amines (although ∼1000 times slower than with thiol groups).[38] In addition, a broad peak at 26139 Da (dimer) was observed.

Cyanogen bromide (CNBr) cleavage of **3a** was performed according to a literature procedure,[34] resulting in conjugate **4a**. Cleavage was carried out after conjugation, since the N-terminal 6 × His tag could be used for the efficient removal of PEG (as described above). Removal of PEG via dialysis turned out to be problematic. The protein conjugate **3a** was dissolved in 70% formic acid (2 mg mL^{-1}), and an equal volume of CNBr (Aldrich) in 70% formic acid (100 mg mL^{-1}) was added, followed by incubation on a rotary arm for 2 days at room temperature in the dark. The sample was dried in a centrifugal dryer at room temperature. The pellet was redissolved in demi-water and dialyzed for 2 days against demi-water using a dialysis membrane (molecular weight cutoff = 3500 Da; Spectra Por). MALDI-TOF: m/z = 8529 Da, main peak (calculated mass for bifunctionalized product: 8538 Da) and a smaller peak with m/z = 10 830 Da (incomplete cleavage).

*[(AG)$_3$EG]$_{10}$-PEG-2000 Conjugate (**3b**).* ^{1}H NMR (400 MHz, H_2O/D_2O 9:1 v/v): The following major signals were assigned: δ = 1.40 (d, 123H, Ala-Hβ), 2.11 (m, 26H, Glu-Hβ), 2.31 (m, 26H, Glu-Hγ), 3.40 (s, 6H, CH_3O), 3.72 (s, 376H, O(CH_2)$_2$O), 4.14 (s, 92H, Gly-Hα), 4.28 (m, 54H, Ala/Glu-Hα). MALDI-TOF: m/z = 15 417 Da (calculated mass for bifunctionalized product: 15 762 Da).

MALDI-TOF after CNBr cleavage (**4b**): m/z = 10 872 Da (broad peak) (calculated mass for bifunctionalized product: 11 098 Da).

*[(AG)$_3$EG]$_{10}$-PEG-5000 Conjugate (**3c**).* ^{1}H NMR (400 MHz, H_2O/D_2O 9:1 v/v): The following major signals were assigned: δ = 1.40 (d, 123H, Ala-Hβ), 2.11 (m, 26H, Glu-Hβ), 2.30 (m, 26H, Glu-Hγ), 3.40 (s, 6H, CH_3O), 3.72 (s, 920H, O(CH_2)$_2$O), 3.97 (s, 92H, Gly-Hα), 4.28 (m, 54H, Ala/Glu-Hα). MALDI-TOF: pre-

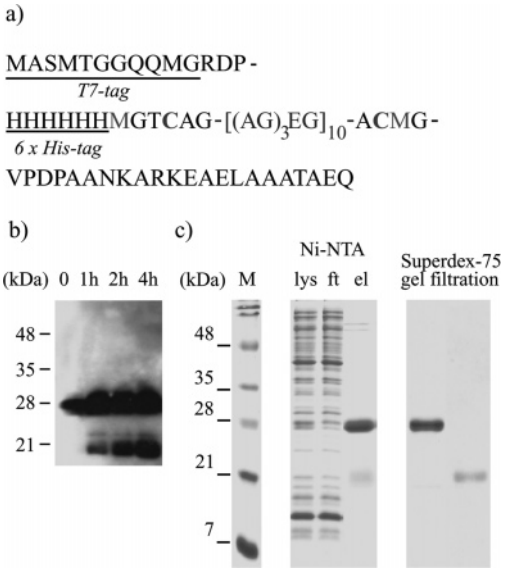

Figure 1. (a) Sequence of $[(AG)_3EG]_{10}$ (**1**) as expressed in *E. coli*. The sequence is flanked by two cysteine residues used for conjugation of poly(ethylene glycol) and two methionine residues for removal of N- and C-terminal amino acids by cyanogen bromide cleavage. (b) Expression of $[(AG)_3EG]_{10}$ followed by immunoblot analysis using mouse monoclonal T7-tag antibody. Whole cell lysates were used. (c) SDS-PAGE analysis of purification of $[(AG)_3EG]_{10}$ by native Ni-NTA chromatography (lys = soluble lysate, ft = flow-through, el = elution) and gel filtration chromatography (Superdex-75). M = molecular weight marker. Proteins were visualized by staining with Coomassie Brilliant Blue R-250.

dominant signal: m/z = 21 552 Da (calculated mass for bifunctionalized product: 21 804 Da). Minor signals: m/z = 16 219 and 26 323 Da (calculated mass for mono- and trifunctionalized product is 16 458 and 27 150 Da, respectively).

MALDI-TOF after CNBr cleavage (**4c**): m/z = 16 890 Da (calculated mass for bifunctionalized product 17 140 Da), 11 589 Da (calculated mass for monofunctionalized product: 11 794 Da) and 9215 Da (not assigned).

*$[(AG)_3EG]_{10}$-ϵ-maleimidocaproic Acid Conjugate (**5**).* ^{1}H NMR (400 MHz, H_2O/D_2O 9:1 v/v): The following major signals were assigned: δ = 1.40 (d, 123H, Ala-Hβ), 2.10 (m, 26H, Glu-Hβ), 2.26 (m, 26H, Glu-Hγ), 3.91 (s, 92H, Gly-Hα), 4.28 (m, 54H, Ala/Glu-Hα).

MALDI-TOF: m/z = 11 588 Da (calculated mass for bifunctionalized product: 11 534 Da), 11 356 Da (calculated mass for monfunctionalized product: 11 323 Da) and 22 215 Da (dimeric product). MALDI-TOF after CNBr cleavage (**6**): m/z = 13 600, 20 233, and 26 842 Da (corresponding to dimeric, trimeric, and tetrameric products, these signals are presumably the result of aggregate formation), 9154 Da (not assigned).

Results and Discussion

Expression and Purification of $[(AG)_3EG]_{10}$ (1). The expression of the β-sheet polypeptide $[(AG)_3EG]_{10}$ with flanking cysteine residues (Figure 1a) was followed by immunoblot analysis using T7 tag mouse monoclonal antibodies (Figure 1b). Two major bands were detected after induction with isopropyl-β-D-thiogalactopyranoside (IPTG), and the upper band with an apparent molecular weight of 28 kDa corresponded to the full-length polypeptide. The actual molecular weight of this polypeptide is 11.1 kDa, as was confirmed by MALDI-TOF analysis. This slow migration on an SDS−polyacrylamide gel has been reported for this sequence before and is also observed for other highly acidic proteins.[30,39] The lower band at the height of the 21 kDa marker which appeared during the expression of **1** was isolated and subsequently analyzed by MALDI-TOF mass spectrometry. It was demonstrated that this band did not correspond to a discrete protein product but was a mixture of truncated products with a molecular weight between 6 and 7 kDa. This molecular weight corresponds to polypeptides with around six repeats of the octapeptide $(AG)_3EG$. The formation of truncated products during the expression of repetitive proteins has been observed previously, e.g., also in the expression of $[(AG)_3EG]_{20}$,[29] and is generally explained as premature termination of translation. The polypeptide was present in the soluble fraction of the lysate and was therefore purified by Ni-NTA chromatography under native conditions. Although the molecular weight difference between the full-length product and the truncated form is relatively small, gel filtration purification using a Superdex-75 column resulted in a successful separation of the two polypeptides (Figure 1c). The isolated yield for the full-length product after dialysis and freeze-drying was ~6 mg L^{-1} of culture.

Conjugation of PEGs and $[(AG)_3EG]_{10}$. A series of conjugates were prepared by coupling of the β-sheet polypeptide **1** with PEGs with number-average molecular weights of 750, 2000, and 5000 g mol^{-1}, leading to compounds **3a**, **3b**, and **3c**, respectively. For that purpose amine-end-functionalized monomethoxy-PEG chains were functionalized with a maleimide group, capable of reacting with the thiol groups of the two cysteine residues located on both sides of the $[(AG)_3EG]_{10}$ sequence (Figure 2). This modification was conveniently performed with ϵ-maleimidocaproic acid, using BOP (benzotriazole-1-yl-oxytris(dimethylamino)phosphonium hexafluorophosphate) as a coupling agent. After reaction for 1 day, the PEGs **2a**, **2b**, and **2c** were purified by gel filtration chromatography with isolated yields of 70−90%.

The preparation procedure for the conjugates is summarized in Figure 3. The free thiol content after dissolution of the purified and freeze-dried polypeptide **1** was determined with Ellman's[35] essay, which indicated that only 5% of the cysteines was in reduced form. Therefore, the oxidized cysteines were reduced using an excess of dithiotreitol (DTT). Initially, it was attempted to remove the excess DTT via dialysis, but this turned out to be too slow, since reoxidation of cysteines was observed. A better alternative was precipitation of the reduced polypeptide with trichloroacetic acid (TCA), which is a commonly used method.[37] The pellet was washed subsequently with 20% and 1% aqueous TCA to remove residual DTT. After dissolution of the pellet in sodium phosphate buffer (pH 6.8), the thiol content was about 75% of the theoretical value (based on weighed-in polypeptide). Conjugation was immediately started by addition of the various maleimide-functionalized PEGs, which were dissolved in the same buffer. Also, a coupling was performed between **1** and ϵ-maleimidocaproic acid, leading to the formation of **5**. To ensure complete functionalization, 5 equiv of maleimide functionality relative to the cysteine residues was used. After 1 day at room temperature, the conjugation reactions were analyzed by SDS-PAGE (Figure 4a). Lane 1 shows the product after conjugation with ϵ-maleimidocaproic acid and a slight downshift was observed in comparison to unreacted polypeptide (lane 5). Surprisingly, also the attachment of PEG-750 (lane 2) resulted in a slightly increased electrophoretic mobility (apparent lower molecular weight), whereas the attachment of longer PEG chains (PEG-2000 and PEG-5000; lane 3 and 4) again resulted in a shift of bands to higher molecular weight. The strange migration behavior on SDS-PAGE gel cannot be explained easily. One has to take into account, however, that the unreacted polypeptide already migrates anomalously slow on gel. Furthermore, particularly for the PEG-

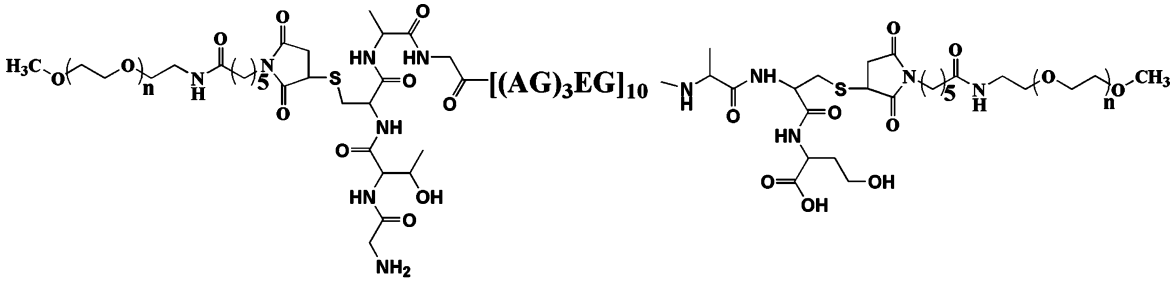

Prepared conjugates:

DP of PEG-block, n =	uncleaved	CNBr cleaved
17	3a	4a
47	3b	4b
115	3c	4c
ε-maleimidocaproic acid	5	6

Figure 2. Structure of ABA triblock copolymer with a central $[(AG)_3EG]_{10}$ polypeptide block and poly(ethylene glycol) (PEG) end blocks prepared via conjugation of maleimide-functionalized PEGs (PEG-750, PEG-2000, and PEG-5000; n = 17, 47, and 115) to N- and C-terminal cysteine residues.

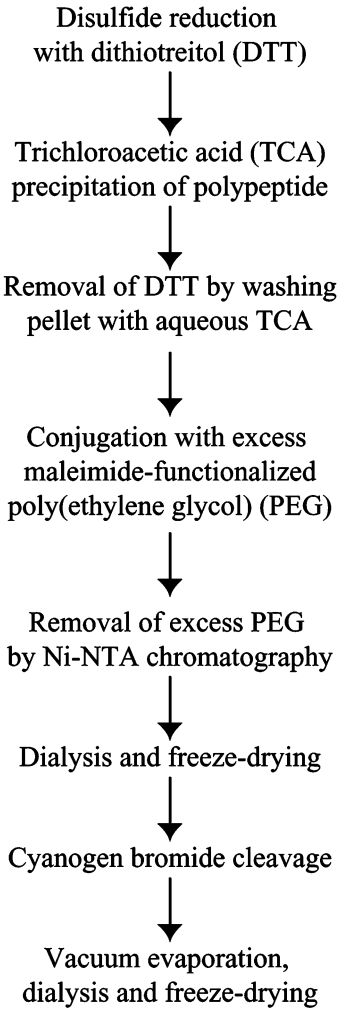

Figure 3. Preparation procedure for poly(ethylene glycol) conjugates of β-sheet polypeptides.

5000 conjugate, higher molecular weight bands were detected. These bands are most likely physically aggregated conjugates, since SDS-PAGE was carried out under reducing conditions (loading buffer contained 2% β-mercaptoethanol). The expected molecular weights for **1** conjugated with two PEG chains of PEG-750, PEG-2000, and PEG-5000 are 13.2, 15.8, and 21.8 kDa, respectively. MALDI-TOF mass spectrometry showed that

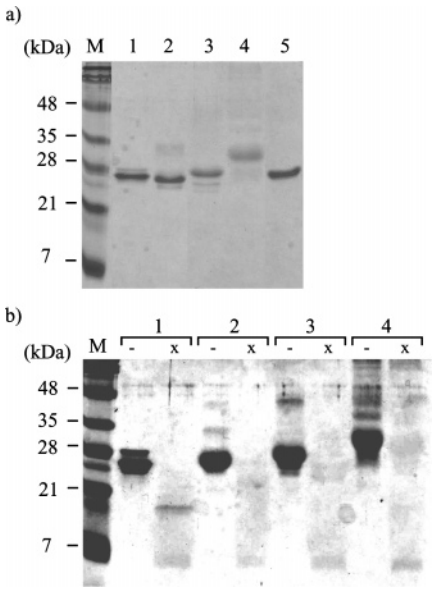

Figure 4. SDS-PAGE analysis of (a) conjugation of $[(AG)_3EG]_{10}$ and ϵ-maleimidocaproic acid (lane 1) PEG-750 (lane 2), PEG-2000 (lane 3), and PEG-5000 (lane 4). Unreacted $[(AG)_3EG]_{10}$ was loaded in lane 5. M = molecular weight marker. (b) Cyanogen bromide (CNBr) cleavage of conjugates of $[(AG)_3EG]_{10}$ and ϵ-maleimidocaproic acid (1), PEG-750 (2), PEG-2000 (3), and PEG-5000 (4). For both the noncleaved samples (−) and the CNBr-cleaved (x) 10 μg was loaded. Polypeptides were visualized by Coomassie Brilliant Blue R-250 staining. To visualize CNBr-cleaved conjugates contrast enhancement was carried out.

the predominant PEG conjugates formed were in agreement with these values. Some impurities could be observed corresponding to monofunctionalized and trifunctionalized product. Trifunctionalization is most likely the result of functionalization of lysine residues or the N-terminus, since the maleimide functionality eventually also reacts with amines (although ~1000 times slower than with thiol groups).[38]

Since the His tag was still present in the PEG conjugates, Ni-NTA column chromatography could be efficiently used to bind the conjugates and remove the excess PEG upon washing, as was monitored by measuring the absorption decrease of the flow-through at 214 nm. After elution of the conjugates from the column, the fractions were dialyzed to remove imidazole and salts. The N- and C-terminal amino acids were subsequently

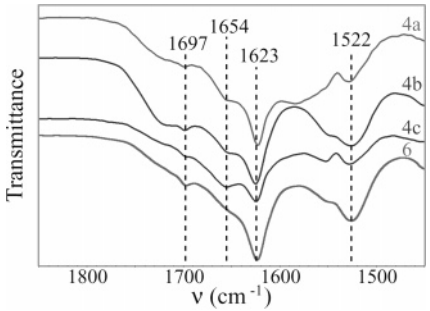

Figure 5. Infrared spectra of crystallized conjugates of $[(AG)_3EG]_{10}$ and PEG-750 (compound **4a**), PEG-2000 (compound **4b**), PEG-5000 (compound **4c**), and ϵ-maleimidocaproic acid (compound **6**). Amide I and II regions are shown. Samples (10 mg mL^{-1}) were dried on the IR crystal prior to measurement.

removed by cyanogen bromide (CNBr) cleavage. After this reaction the capability of staining the conjugates with Coomassie was almost completely lost (Figure 4b). Only after contrast enhancement, vague bands could be detected at slightly lower molecular weight than the original conjugates (compare lanes − and ×). With contrast enhancement and at these high loadings of 10 μg the aggregated, high molecular weight conjugates can be detected clearly. Furthermore, for the conjugate with ϵ-maleimidocaproic acid two bands are present before cyanogen bromide cleavage. The upper band was located at the height of unreacted polypeptide (visible in Figure 4a) but could also correspond to polypeptide monofunctionalized with ϵ-maleimidocaproic acid. The peaks found by MALDI-TOF mass spectrometry were in reasonable agreement with the expected molecular weights of 8.5, 10.1, and 17.1 kDa for conjugates of PEG-750, PEG-2000, and PEG-5000, respectively (see Supporting Information).

Effect of PEG Chain Length on β-Sheet Formation, Studied by Infrared Spectroscopy. Vapor diffusion of methanol into a 10 mg mL^{-1} solution of the various PEG conjugates of $[(AG)_3EG]_{10}$ (**3a**−**c** and **4a**−**c**) in 70% formic acid was carried out for 2 days to induce crystallization. The viscosity of the gelated samples decreased with increasing length of the PEG chain. This could be expected, considering the smaller relative portion of the aggregating β-sheet polypeptide. The effect of conjugation of PEG and its chain length on the secondary structure of $[(AG)_3EG]_{10}$ was investigated by infrared spectroscopy. For this purpose the samples were dried on the surface of the IR crystal. Figure 5 shows the IR spectra for gelated conjugates of $[(AG)_3EG]_{10}$ with ϵ-maleimidocaproic acid, PEG-750, PEG-2000, and PEG-5000 (**6**, **4a**, **4b**, and **4c** respectively, all CNBr cleaved). The frequencies of the amide I (80% C═O stretch vibration) and amide II (60% N−H bend vibration) were used for indication of the secondary structure of the polypeptide block.[40−42] The IR spectra are very similar, showing three bands around 1697, 1654, and 1623 cm^{-1} in the amide I region as well as a band around 1522 cm^{-1} in the amide II region. The strong bands at 1623 and 1522 cm^{-1} and the weak band at 1697 cm^{-1} are indicative for the antiparallel β-sheet conformation. The amide I band around 1654 cm^{-1} (and also the amide II bands around 1550 cm^{-1}, not indicated) indicates that some fraction of the polypeptide chain has adopted a secondary structure different from the antiparallel β-sheet. This amide I component has been assigned previously to reverse turns of the β- or γ-type[30] but may also (partly) result from a random coil/α-helical conformation. It has also been assigned to the silk I structure.[31] This component becomes relatively stronger with longer PEG chains. Overall, however, we can conclude that the antiparallel β-sheet structure is retained upon attachment of PEG and that the spectra do not change significantly for the varying PEG chain lengths.

Aggregation Behavior of PEG−Protein Conjugates Studied by Transmission Electron Microscopy (TEM) and Atomic Force Microscopy (AFM). TEM and AFM studies were carried out to investigate the microstructure of the crystallized β-sheet conjugates. All samples were prepared by placing a carbon-coated TEM grid on a droplet of a suspension of the conjugate. After drying, the samples were shadowed with platinum. For the $[(AG)_3EG]_{10}$−PEG-750 conjugate a clear fibrillar microstructure was observed only for the uncleaved variant, **3a** (Figure 6a). For CNBr-cleaved $[(AG)_3EG]_{10}$−PEG-750 conjugate (**4a**) single fibrils were difficult to distinguish because of dense coverage of the grid (Figure 6b). Attempts to improve visualization of these fibrils by diluting the sample and by applying negative staining (uranyl acetate and phosphotungstic acid) did not succeed. For conjugates of $[(AG)_3EG]_{10}$ with PEG-2000 (**3b** and **4b**) and PEG-5000 (**3c** and **4c**) we were not able to visualize any structure for samples crystallized from a 10 mg mL^{-1} solution. Only for the uncleaved samples (**3b** and **3c**) crystallized from a more dilute, 1 mg mL^{-1}, solution were irregular, micrometer-sized aggregates visible (Figure 6c,d). This morphology is alike the spherulitic texture for a recombinant silklike protein polymer reported by Anderson and co-workers[43] and is also commonly seen in thin films of semicrystalline polymers.[44] A zoomed-in image of these aggregates (inset) showed the presence of a fibrillar morphology. The dimensions of the fibrils could not be determined, in contrast to the previously reported conjugate of PEG-750 with a polypeptide block consisting of 20 instead of 10 repeats of -$[(AG)_3EG]$-.[29]

For $[(AG)_3EG]_{10}$ conjugated to ϵ-maleimidocaproic acid no fibrillar structure or other morphology could be observed (Figure 6e). This is likely to reflect the larger extent of physical cross-linking for this conjugate as a result of the increased interaction between the β-sheet polypeptides.

Figure 7 shows representative AFM images of crystallized samples for the four different CNBr-cleaved conjugates of $[(AG)_3EG]_{10}$ after drop-casting on a mica surface (**6**, **4a**, **4b**, and **4c**). For the conjugate with ϵ-maleimidocaproic acid (**5**) no fibrillar structures were observed, but instead a morphology with pores of ∼50 nm was found (Figure 7a). The attachment of the various PEGs resulted in all cases in a fibrillar microstructure (Figure 7b−f). Whereas no microstructure for **4b** and **4c** could be visualized using TEM, AFM was able to clearly demonstrate the presence of fibrils. Micrometer-long fibrils were observed, especially for **4a** and **4b**. For $[(AG)_3EG]_{10}$ conjugated with PEG-5000 (**4c**), the fibrillar structure seemed to be less defined (Figure 7e), and diluting this sample with methanol in order to get images of separate fibrils resulted in short fibril fragments (Figure 7f). Presumably, conjugation of longer PEG chains hinders formation of long fibrils. No differences in fibrillar heights could be established between the conjugates of PEG-750, PEG-2000, and PEG-5000 conjugates. A relatively broad distribution in the measured values was obtained of 1.9 ± 0.7, 2.2 ± 0.3, and 2.4 ± 0.9 nm for the respective conjugates. The difference in TEM and AFM observations for the PEG-2000 and PEG-5000 conjugates cannot be explained easily. As was already observed for the $[(AG)_3EG]_{10}$−PEG-750 conjugate, clear visualization of the fibrillar structure was only obtained for the noncleaved sample, where fibrils were aligned. Since the samples were applied to the surface for TEM and AFM analysis (carbon and mica, respectively) after crystallization (and presumably fibril formation) in a similar procedure, no major differences would be expected. It seems more likely that the

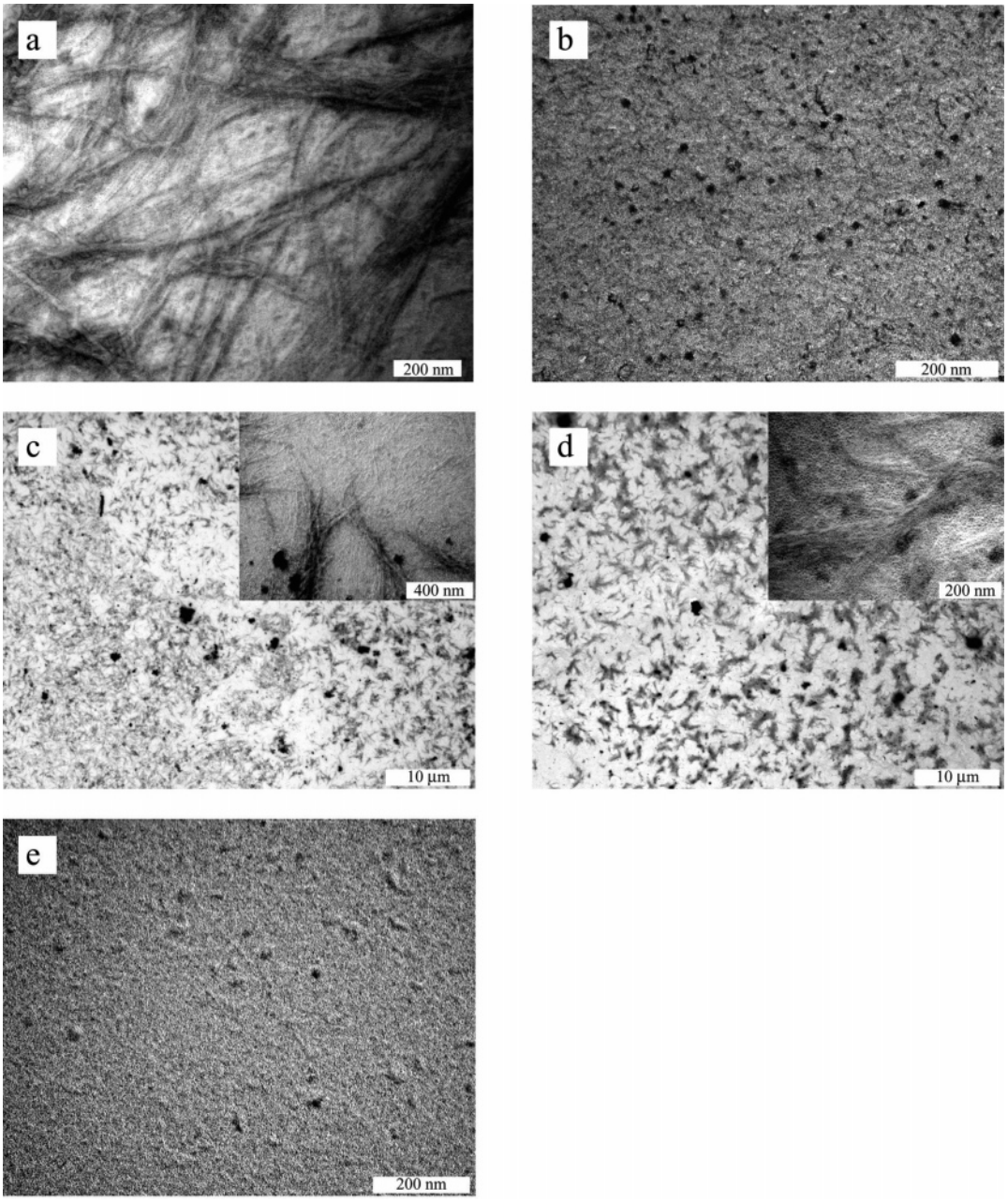

Figure 6. TEM micrographs of crystallized $[(AG)_3EG]_{10}$ polypeptides with conjugated poly(ethylene glycols) of 750, 2000, and 5000 g mol^{-1}. (a) Noncleaved $[(AG)_3EG]_{10}$ conjugated to PEG-750 (compound **3a**), (10 mg mL^{-1}); (b) CNBr-cleaved $[(AG)_3EG]_{10}$ conjugated to PEG-750 (10 mg mL^{-1}) (compound **4a**); (c) noncleaved $[(AG)_3EG]_{10}$ conjugated to PEG-2000 (1 mg mL^{-1}) (compound **3b**); (d) noncleaved $[(AG)_3EG]_{10}$ conjugated to PEG-5000 (1 mg mL^{-1}) (compound **3c**); (e) CNBr-cleaved $[(AG)_3EG]_{10}$ conjugated to ϵ-maleimidocaproic acid (1 mg mL^{-1}) (compound **6**).

resolution of TEM analysis was the limiting factor as a result of the grain size of the platinum particles used for shadowing.

Discussion

Folding of protein **1** conjugated to PEG chains of different length leads in all studied cases to the designed β-sheet conformation, as evidenced by infrared spectroscopy. Although the resolution of TEM in most cases was too low to observe fibrillar structure, AFM proved to be well suited for structural identification. The fact that fibrils formed from uncleaved samples are better visualized with TEM than the cleaved products can be a result of the higher ability for alignment of the former structures, which would make structural characterization more convenient. This improved alignment was clearly observed with TEM for the $[(AG)_3EG]_{20}$−PEG-750 conjugate previously reported.[29]

For the $[(AG)_3EG]_{10}$−PEG-2000 conjugate still well-defined fibrils are observed, whereas after attachment of PEG-5000 no long fibrils are present. The conjugated polymers therefore do not interfere with the folding process, but they do have an effect on the ease of formation of fibrillar assemblies. Although the β-sheet elements prove to be powerful assembly units, when a certain PEG chain length is reached β-sheet stacking is limited. The radius of gyration of the PEG-chains can be estimated to be 8, 15, and 26 Å for PEG-750, PEG-2000, and PEG-5000, respectively.[45] When a calculated width of the β-sheet is taken into account of 4.3 nm, it is clear that especially with PEG 5000 the size of the PEG chain is larger than the polypeptide structure, and therefore shielding can occur to some extent, preventing the polypeptide from interacting. In the other two cases the PEG chains are smaller or of equal size when compared to the polypeptide, and steric hindrance becomes much less obvious,

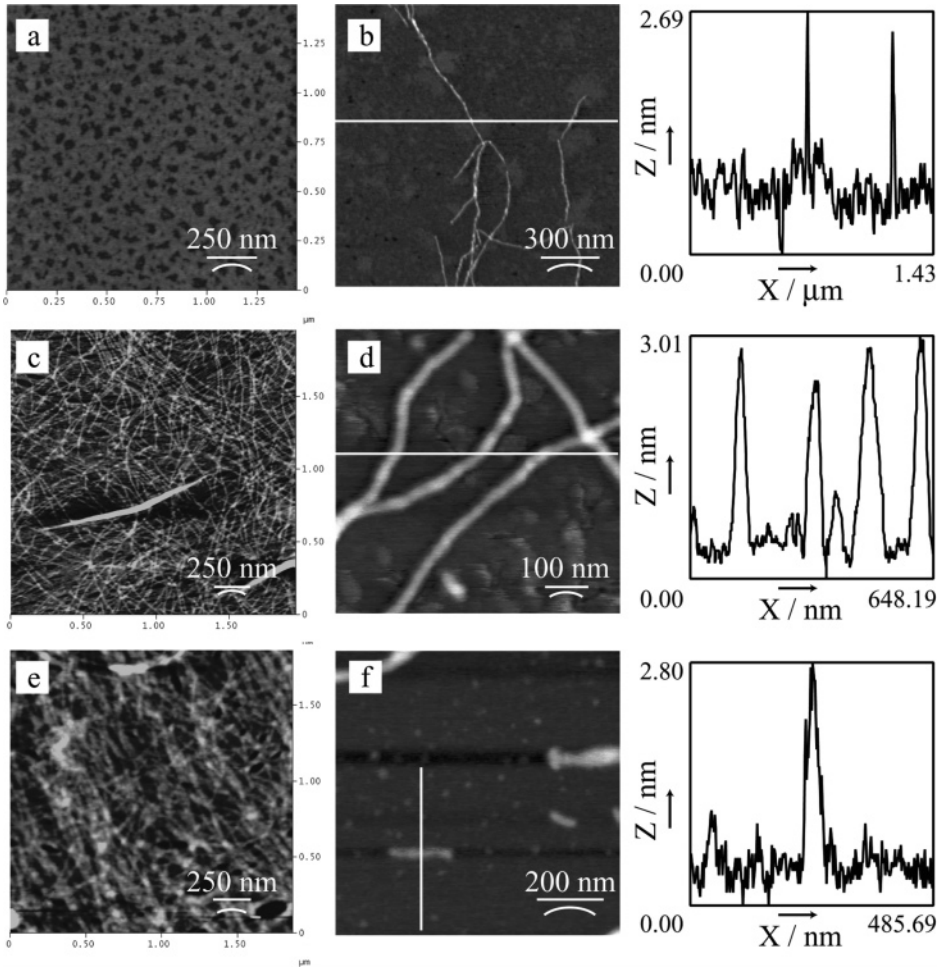

Figure 7. Atomic force microscopy image of dried films of $[(AG)_3EG]_{10}$ conjugated with (a) ϵ-maleimidocaproic acid (compound **6**), (b) PEG-750 (compound **4a**), (c, d) PEG-2000 (compound **4b**), and (e, f) PEG-5000 (compound **4c**). For (b), (d), and (f) a height profile is depicted. All samples were cleaved with cyanogen bromide. Crystallized samples were diluted with methanol and applied on the mica surface by drop-casting (concentrations in the range 0.01−0.1 mg mL^{-1}).

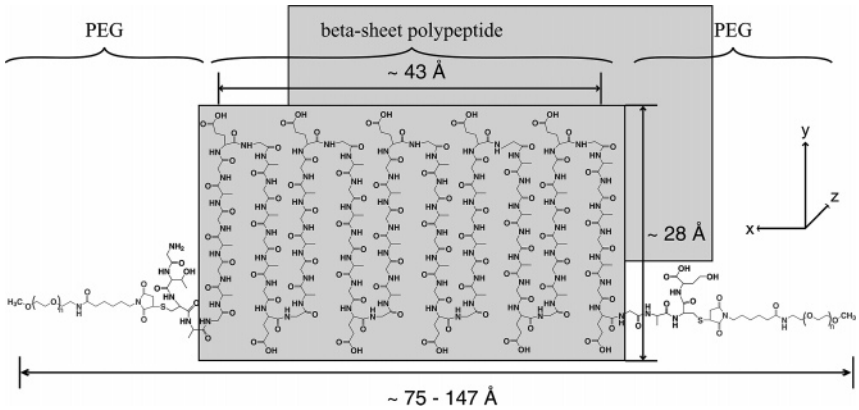

Figure 8. Proposed model for the organization of triblock copolymers of a central $[(AG)_3EG]_{10}$ polypeptide block and PEG end blocks within fibrils. The model comprises folded β-sheets stacked along the *z*-axis, leading to fibril formation (perpendicular to the plane of the page). Antiparallel β-strands are formed (x = hydrogen-bonding direction, y = chain axis direction) with glutamic acid residues at the fibril surface. PEG chains hinder further lateral aggregation by preventing hydrogen bonding along the *x*-axis. Depending on the molecular weight of the PEG chain used (with radius of gyration from ~8 Å for PEG-750 to 26 Å for PEG-5000), widths of ~75−147 Å are expected.

which is confirmed by our measurements. Polymer attachment, however, remains necessary for fibril formation, as is demonstrated by the fact that crystallized conjugates **5** and **6** do not show the fibrillar morphologies.

With the chosen crystallization method, the PEG blocks are expected to stay dissolved, since methanol is a good solvent for this polymer.[45] Fibril formation in the β-sheet stacking direction results in an assembly in which the hydrophobic β-sheet surfaces are shielded from methanol, whereas the PEG chains are in contact with the solvent. This proposed assembly model in which fibril formation occurs in the β-sheet stacking direction and the number of -$[(AG)_3EG]$- repeats determines the fibrillar width (Figure 8) was supported previously by combined TEM and AFM measurements and further substantiated by the results presented here.[29] Based on this model, the expected values for the width of the $[(AG)_3EG]_{10}$ and $[(AG)_3EG]_{20}$

polypeptide blocks are 4.3 and 8.9 nm, respectively.[30] The total fibril diameter for the $[(AG)_3EG]_{10}$−PEG-750 and $[(AG)_3EG]_{20}$−PEG-750 conjugates can be estimated to be 7.5 and 12.1 nm, respectively, when it is assumed that the PEG chain can adopt a random coil structure. The fibrillar width (or, more accurately expressed, a repeating distance) of ∼12 nm could be measured for the $[(AG)_3EG]_{20}$−PEG-750 conjugate with TEM. Unfortunately, the low resolution of the TEM pictures of the $[(AG)_3EG]_{10}$−PEG-750 conjugate only supply us with the qualitative information that the fibrillar width is decreased.

With respect to height a clearer picture can be observed. AFM analysis showed the same height values of ∼2 nm for all conjugates of $[(AG)_3EG]_{10}$ and $[(AG)_3EG]_{20}$, which are somewhat lower than the calculated height of 2.8 nm. It has to be noted, however, that AFM measurements do not give absolute height values as a result of possible deformation caused by the tip's pressure and the influence of air humidity.[46]

For an alternative assembly arrangement, in which cylindrical instead of rectangular fibrils are formed, as reported for PEG conjugates of small β-sheet peptides by a number of groups,[23,26] changing the PEG chain length is expected to be reflected in the height values as measured by AFM. In our case we seem to be able to exclude such an arrangement, since no difference in height could be established for the varying conjugates, which supports the proposed assembly model.

Although as a final proof of the β-sheet fibril assembly the confinement of glutamic acid residues at the fibrillar surface should be demonstrated, this class of polypeptide−polymer hybrids has the potential to control height and surface functionality of the fibrils and could be useful as well-defined building blocks in nanometer-sized materials.

Conclusions

We have demonstrated the efficient preparation of a series of ABA triblock copolymers composed of a central poly-$[(AG)_3EG]$ block and various PEG end blocks via conjugation of maleimide-functionalized PEGs to two cysteine residues on the N- and C-terminal side of the polypeptide block. In the future diffraction experiments are planned to obtain more information on the regular arrangement of the β-sheet polypeptides in the fibrils as well as possible crystallinity of the PEG blocks after drying. Then functionalization of the fibrils with chemical functionalities can be carried out e.g. for the preparation of conducting nanowires or as template for biomineralization.

Acknowledgment. The authors acknowledge Huub Geurts for his help with transmission electron microscopy.

Supporting Information Available: MALDI-TOF mass and ^{1}H NMR spectra. This material is available free of charge via the Internet at http://pubs.acs.org.

References and Notes

(1) Sleytr, U. B.; Schuster, B.; Pum, D. *IEEE Eng. Med. Biol. Magn.* **2003**, *22*, 140.

(2) Scheibel, T.; Parthasarathy, R.; Sawicki, G.; Lin, X. M.; Jaeger, H.; Lindquist, S. L. *Proc. Natl. Acad. Sci. U.S.A.* **2003**, *100*, 4527.

(3) Yeates, T. O.; Padilla, J. E. *Curr. Opin. Struct. Biol.* **2002**, *12*, 464.

(4) Dotan, N.; Arad, D.; Frolow, F.; Freeman, A. *Angew. Chem., Int. Ed.* **1999**, *38*, 2363.

(5) Ringler, P.; Schulz, G. E. *Science* **2003**, *302*, 106.

(6) Aggeli, A.; Bell, M.; Carrick, L. M.; Fishwick, C. W. G.; Harding, R.; Mawer, P. J.; Radford, S. E.; Strong, A. E.; Boden, N. *J. Am. Chem. Soc.* **2003**, *125*, 9619.

(7) Marini, D. M.; Hwang, W.; Lauffenburger, D. A.; Zhang, S. G.; Kamm, R. D. *Nano Lett.* **2002**, *2*, 295.

(8) Lu, K.; Jacob, J.; Thiyagarajan, P.; Conticello, V. P.; Lynn, D. G. *J. Am. Chem. Soc.* **2003**, *125*, 6391.

(9) Santoso, S.; Hwang, W.; Hartman, H.; Zhang, S. G. *Nano Lett.* **2002**, *2*, 687.

(10) Colfer, S.; Kelly, J. W.; Powers, E. T. *Langmuir* **2003**, *19*, 1312.

(11) Rapaport, H.; Moller, G.; Knobler, C. M.; Jensen, T. R.; Kjaer, K.; Leiserowitz, L.; Tirrell, D. A. *J. Am. Chem. Soc.* **2002**, *124*, 9342.

(12) Powers, E. T.; Yang, S. I.; Lieber, C. M.; Kelly, J. W. *Angew. Chem., Int. Ed.* **2002**, *41*, 127.

(13) Schneider, J. P.; Pochan, D. J.; Ozbas, B.; Rajagopal, K.; Pakstis, L.; Kretsinger, J. *J. Am. Chem. Soc.* **2002**, *124*, 15030.

(14) Aggeli, A.; Bell, M.; Boden, N.; Carrick, L. M.; Strong, A. E. *Angew. Chem., Int. Ed.* **2003**, *42*, 5603.

(15) Zhang, S.; Holmes, T. C.; Lockshin, C.; Rich, A. *Proc. Natl. Acad. Sci. U.S.A.* **1993**, *90*, 3334.

(16) Zhang, S. G.; Zhao, X. J. *J. Mater. Chem.* **2004**, *14*, 2082.

(17) West, M. W.; Wang, W. X.; Patterson, J.; Mancias, J. D.; Beasley, J. R.; Hecht, M. H. *Proc. Natl. Acad. Sci. U.S.A.* **1999**, *96*, 11211.

(18) Xu, G.; Wang, W.; Groves, J. T.; Hecht, M. H. *Proc. Natl. Acad. Sci. U.S.A.* **2001**, *98*, 3652.

(19) Brown, C. L.; Aksay, I. A.; Saville, D. A.; Hecht, M. H. *J. Am. Chem. Soc.* **2002**, *124*, 6846.

(20) Goeden-Wood, N. L.; Keasling, J. D.; Muller, S. J. *Macromolecules* **2003**, *36*, 2932.

(21) Schlaad, H.; Antonietti, M. *Eur. Phys. J. E* **2003**, *10*, 17.

(22) Gallot, B. *Prog. Polym. Sci.* **1996**, *21*, 1035.

(23) Burkoth, T. S.; Benzinger, T. L. S.; Urban, V.; Lynn, D. G.; Meredith, S. C.; Thiyagarajan, P. *J. Am. Chem. Soc.* **1999**, *121*, 7429.

(24) Burkoth, T. S.; Benzinger, T. L. S.; Jones, D. N. M.; Hallenga, K.; Meredith, S. C.; Lynn, D. G. *J. Am. Chem. Soc.* **1998**, *120*, 7655.

(25) Rosler, A.; Klok, H. A.; Hamley, I. W.; Castelletto, V.; Mykhaylyk, O. O. *Biomacromolecules* **2003**, *4*, 859.

(26) Hamley, I. W.; Ansari, A.; Castelletto, V.; Nuhn, H.; Rosler, A.; Klok, H. A. *Biomacromolecules* **2005**, *6*, 1310.

(27) Rathore, O.; Sogah, D. Y. *Macromolecules* **2001**, *34*, 1477.

(28) Rathore, O.; Sogah, D. Y. *J. Am. Chem. Soc.* **2001**, *123*, 5231.

(29) Smeenk, J. M.; Otten, M. B. J.; Thies, J.; Tirrell, D. A.; Stunnenberg, H. G.; van Hest, J. C. M. *Angew. Chem., Int. Ed.* **2005**, *44*, 1968.

(30) Krejchi, M. T.; Atkins, E. D. T.; Waddon, A. J.; Fournier, M. J.; Mason, T. J.; Tirrell, D. A. *Science* **1994**, *265*, 1427.

(31) Chen, C. C.; Krejchi, M. T.; Tirrell, D. A.; Hsu, S. L. *Macromolecules* **1995**, *28*, 1464.

(32) Krejchi, M. T.; Atkins, E. D. T.; Fournier, M. J.; Mason, T. L.; Tirrell, D. A. *J. Macromol. Sci., Pure Appl. Chem.* **1996**, *A33*, 1389.

(33) Krejchi, M. T.; Cooper, S. J.; Deguchi, Y.; Atkins, E. D. T.; Fournier, M. J.; Mason, T. L.; Tirrell, D. A. *Macromolecules* **1997**, *30*, 5012.

(34) Ausubel, F.; Brent, R.; Kingston, R.; Moore, D.; Seidman, J.; Smith, J.; Struhl, K. *Current Protocols in Molecular Biology*; John Wiley & Sons: New York, 1999; Vol. 3.

(35) Ellman, G. L. *Arch. Bioch. Biophys.* **1959**, *82*, 70.

(36) Bodanszky, M. B. A. *The Practise of Peptide Synthesis*, 2nd ed.; Springer-Verlag: Berlin, 1994.

(37) Sambrook, J.; Fritsch, E. F.; Maniatis, T. *Molecular Cloning: A Laboratory Manual*, 2nd ed.; Cold Spring Laboratory Press: Cold Spring, 1989.

(38) Hermanson, G. T. *Bioconjugate Techniques*; Academic Press: San Diego, 1996.

(39) McGrath, K. P.; Fournier, M. J.; Mason, T. L.; Tirrell, D. A. *J. Am. Chem. Soc.* **1992**, *114*, 727.

(40) Miyazawa, M.; Blout, E. R. *J. Am. Chem. Soc.* **1960**, *83*, 712.

(41) Krimm, S.; Bandekar, J. *Adv. Protein Chem.* **1986**, *38*, 181.

(42) Pelton, J. T.; McLean, L. R. *Anal. Biochem.* **2000**, *277*, 167.

(43) Anderson, J. P.; Cappello, J.; Martin, D. C. *Biopolymers* **1994**, *34*, 1049.

(44) Geil, P. H. *Polymer Single Crystals*; R.E. Krieger Pub. Co.: Huntington, NY, 1973.

(45) Kinugasa, S.; Nakahara, H.; Kawahara, J. I.; Koga, Y.; Takaya, H. *J. Polym. Sci., Part B: Polym. Phys.* **1996**, *34*, 583.

(46) *Atomic Force Microscopy: Biomedical Methods and Applications*; Humana Press: Totowa, NJ, 2004; Vol. 242.

MA0521654